IEICE TRANS. COMMUN., VOL.E98–B, NO.11 NOVEMBER 2015

PAPER

Estimating Living-Body Location Using Bistatic MIMO Radar in Multi-Path Environment

Keita KONNO[†], *Student Member*, Naoki HONMA[†a)], *Member*, Dai SASAKAWA[†], *Student Member*, Kentaro NISHIMORI[††], *Senior Member*, Nobuyasu TAKEMURA[†††], Tsutomu MITSUI[††††], *and* Yoshitaka TSUNEKAWA[†], *Members*

SUMMARY This paper proposes a method that uses bistatic Multiple-Input Multiple-Output (MIMO) radar to locate living-bodies. In this method, directions of living-bodies are estimated by the MUltiple SIgnal Classification (MUSIC) method at the transmitter and receiver, where the Fourier transformed virtual Single-Input Multiple-Output (SIMO) channel matrix is used. Body location is taken as the intersection of the two directions. The proposal uses a single frequency and so has a great advantage over conventional methods that need a wide frequency band. Also, this method can be used in multipath-rich environments such as indoors. An experiment is performed in an indoor environment, and the MIMO channels yielded by various subject numbers and positions are measured. The result indicates that the proposed method can estimate multiple living-body locations with high accuracy, even in multipath environments.

key words: *MIMO, living-body location, DOA estimation, microwave sensor, array antenna*

1. Introduction

In recent years, the increase in the elderly living alone has become a key issue in several countries. Because of this, accidental falls and lonely death have become social problems, and calls for a safety confirmation system for the elderly are growing. The use of video cameras and electrocardiograms (ECG) are mentioned as the conventional approaches to safety confirmation [1]. However, the former has problems with privacy violation, the heavy burdens placed on the monitor, and its restriction to line-of-sight (LOS) situations. The latter is handicapped by the physical and mental burdens caused by continual and direct contact of the probe on the human body. Therefore, a safety confirmation system that can monitor the health and the position of the living-body without these problems is needed.

An attractive solution is to use microwave sensors for safety confirmation [2]–[9]. This approach does not violate privacy, and body contact is not needed. A vital sign observation method that uses Multiple-Input Multiple-Output (MIMO) technology was proposed by Nango et al. [8]. This method can detect vital signs even if the antenna and the living-body are widely separated (about 6.0 m). However, the location of the living-body cannot be estimated.

MIMO radar in the microwave band has been mentioned as a localization method [10]. However, localization methods for vital sign sources using MIMO radar have not been studied adequately. Furthermore, estimation accuracy is degraded in multi-path environments due to multi-path reflections when we use the radar in indoor environments. To solve this problem, Adib et al. proposed to estimate the location of living-bodies by using Frequency-Modulated Continuous-Wave (FMCW) radar containing multiple transmitting and receiving antennas [9]. In this method, the distance between antennas and targets is measured by estimating the round trip time-of-flight (TOF), and target locations are estimated by applying the relationship between this distance and multiple antenna locations. However, this method requires wide bandwidth, 1.79 GHz (from 5.46 GHz to 7.25 GHz) to obtain adequate distance resolution. Moreover, this method has the problem that propagation information in static environments is essential to eliminate unwanted components such as waves reflected from walls, non-living objects, and so on. Because of this, it is expected that estimation accuracy will be significantly degraded if the positions of furniture in the monitoring area are changed.

The authors have proposed a method of estimating living-body direction that uses a single frequency in multi-path environments [11]. In actual multi-path environments, estimating living-body direction has been difficult because of the existence of unwanted components as described above. Our proposal uses the Fourier transformed channel matrix, which is observed by a Single-Input Multiple-Output (SIMO) radar, and the channel components altered by the living-body are extracted. Living-body direction is estimated by applying the MUltiple SIgnal Classification (MUSIC) method [12] to the extracted channel components. Using a single frequency for estimating living-body direction is superior to conventional localization methods that need wide frequency bandwidth. Though this method can estimate living-body direction even in an indoor environment, living-body location could not be determined since the distance between the antenna and living-body could not be estimated.

The authors also proposed a method of living-body localization using bistatic MIMO radar as an extension of the work [13], [14]. The MIMO configuration can estimate

Manuscript received January 28, 2015.
Manuscript revised July 11, 2015.

[†]The authors are with Graduate School of Engineering, Iwate University, Morioka-shi, 020-8551 Japan.
[††]The author is with Graduate School of Science and Technology, Niigata University, Niigata-shi, 950-2181 Japan.
[†††]The author is with Nippon Institute of Technology, Saitama-ken, 345-8501 Japan.
[††††]The author is with the Samsung R&D Institute Japan CO. LTD, Yokohama-shi, 230-0027 Japan.
a) E-mail: honma@m.ieice.org

DOI: 10.1587/transcom.E98.B.2314

both Direction of Departure (DOD) and Direction of Arrival (DOA) at the same time. In this method, living-body directions are estimated at the transmitter and receiver, and living-body location is estimated as the intersection of these directions. When multiple targets exist, however, multiple living-body directions are estimated at the same time but incorrectly because false images are generated. Also, the transmitter and receiver directly face each other. With this antenna arrangement, no intersection can be found for a target standing directly between the transmitting and receiving antennas. The bistatic MIMO radar suitable for multiple living-bodies has been introduced by authors [15], and some fundamental results have been shown. Nevertheless, the estimation performance was not sufficiently evaluated in [13]–[15].

In this paper, a method that uses bistatic MIMO radar to localize multiple living-bodies is presented and evaluated. In this method, living-body directions at transmitting and receiving antennas are estimated by applying the MUSIC method to the fluctuating components extracted from virtual SIMO channels, and localization is performed by finding the intersection points of these two directions. Multiple target locations can be estimated through the use of the MUSIC method utilizing both DOD and DOA as functions. This method uses a single frequency, and static channels are not necessary. Moreover, the antennas are angled 45 degrees into the monitoring area to virtually eliminate dead zones. Experiments are carried out in an indoor environment to show the effectiveness of the proposed method. The results demonstrate that this method can estimate multiple living-body locations even in multi-path environments.

2. Method of Estimating Living-Body Location

Figure 1 shows the concept of the proposed method. This study uses bistatic MIMO radar with an N element linear array transmitter and an M element linear array receiver. θ_{Tx} and θ_{Rx} are the living-body directions of target x at the transmitter and the receiver, respectively. Target x is located at the intersection of θ_{Tx} and θ_{Rx}. θ_{Tx} and θ_{Rx} are estimated by MUSIC method which is a DOA estimation method. However, in multi-path environments, localization is difficult because of unwanted paths such as the direct path, the waves scattered from walls, non-living objects, and so on.

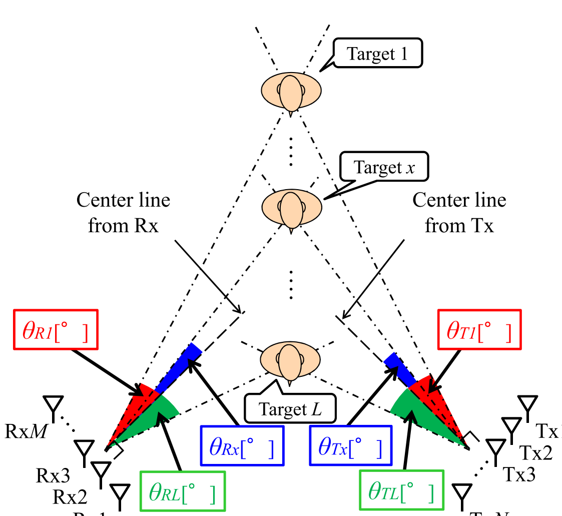

Fig. 1 Concept of living-body localization method.

To realize localization, our method first excludes the unwanted components and observes only the fluctuating components created by human body motion. The principle of the method is reviewed below [15].

In an indoor environment where there are L targets, the measured $M{\times}N$ time-variant MIMO channel is expressed as,

$$\boldsymbol{H}(t) = \begin{pmatrix} h_{11}(t) & \dots & h_{1N}(t) \\ \vdots & \ddots & \vdots \\ h_{M1}(t) & \dots & h_{MN}(t) \end{pmatrix}, \tag{1}$$

where, h_{mn} is the complex channel response from transmitter n to receiver m, and t represents the time of channel observation. $M{\times}N$ bistatic MIMO radar can be considered as $MN{\times}1$ virtual SIMO radar [10]. Here, the $M{\times}N$ MIMO channel matrix, which encompasses the target, is expressed as the $MN{\times}1$ virtual SIMO channel. This is expressed as,

$$\boldsymbol{h}(t) = [h_{11}(t), \cdots, h_{M1}(t), \cdots, h_{MN}(t)]^T, \tag{2}$$

where, $\{\cdot\}^T$ means transposition. While DOD and DOA can be estimated using this virtual SIMO channel, estimating living-body location is difficult because of the existence of unwanted path components. To solve this problem, this study calculates the frequency response matrix by Fourier transformation of the time-variant virtual SIMO channel as expressed by,

$$\boldsymbol{F}(f) = [F_{11}(f), \cdots, F_{M1}(f), \cdots, F_{MN}(f)]^T. \tag{3}$$

Using the frequency response matrix, the correlation matrix, $\boldsymbol{R}_F$, is expressed as,

$$\boldsymbol{R}_F = \overline{\boldsymbol{F}(f)^H \boldsymbol{F}(f)} \quad (f_1 \leq f \leq f_2), \tag{4}$$

where, $\{\cdot\}^H$ means complex conjugate transposition and $\overline{\{\cdot\}}$ represents the averaging operator. f_1 and f_2 delineate the frequency range that encompasses the vital sign effects. By eigenvalue decomposition, $\boldsymbol{R}_F$ is expressed as,

$$\boldsymbol{R}_F = \boldsymbol{U}_F \boldsymbol{\Lambda}_F \boldsymbol{U}_F^H, \tag{5}$$

where, $\boldsymbol{U}_F$ and $\boldsymbol{\Lambda}_F$ represent the eigenvector and the diagonal matrix representing eigenvalues, respectively. They are expressed as,

$$\boldsymbol{U}_F = [\boldsymbol{u}_{F1}, ..., \boldsymbol{u}_{FL}, ..., \boldsymbol{u}_{FMN}], \tag{6}$$

$$\boldsymbol{\Lambda}_F = \mathrm{diag}([\lambda_{F1}, ..., \lambda_{FL}, ..., \lambda_{FMN}]). \tag{7}$$

At this time, the eigenvalues, $\boldsymbol{\Lambda}_F$, are related as follows,

$$\lambda_{F1} \geq \cdots \geq \lambda_{FL} > \lambda_{FL+1} = \cdots = \lambda_{FMN} = \sigma_f^2, \tag{8}$$

where, σ_f^2 represents the expected value of the energy of the channel fluctuation component caused by the influence of noise. The eigenvector corresponding to noise, $[\boldsymbol{u}_{FL+1}, \ldots, \boldsymbol{u}_{FMN}]$, is expressed as $\boldsymbol{U}_N$. $\boldsymbol{U}_N$ are the vectors directing nulls to the signal from the target. Also, the steering vector corresponding to the virtual SIMO channel is called the virtual MIMO steering vector and is expressed as,

$$\boldsymbol{a}(\theta_T, \theta_R) = \boldsymbol{a}_t(\theta_T) \otimes \boldsymbol{a}_r(\theta_R), \tag{9}$$

$$\boldsymbol{a}_t(\theta_T) = [1, e^{-j\frac{2\pi}{\lambda}d_t \sin\theta_T}, \cdots, e^{-j\frac{2\pi}{\lambda}d_t(N-1)\sin\theta_T}]^T, \tag{10}$$

$$\boldsymbol{a}_r(\theta_R) = [1, e^{-j\frac{2\pi}{\lambda}d_r \sin\theta_R}, \cdots, e^{-j\frac{2\pi}{\lambda}d_r(M-1)\sin\theta_R}]^T, \tag{11}$$

where, $\boldsymbol{a}_t(\theta_T)$ and $\boldsymbol{a}_r(\theta_R)$ are the steering vectors at the transmitting and receiving side and represent the plane wave from θ_T and θ_R directions, respectively. $\otimes$ represents the Kronecker product, λ represents wavelength, and d_t and d_r are the element spacing of transmitter and receiver, respectively. By utilizing the eigenvector corresponding to noise, $\boldsymbol{U}_N$, and the virtual MIMO steering vector, $\boldsymbol{a}(\theta_T, \theta_R)$, the evaluation function of the MUSIC method (MUSIC spectrum) is calculated as,

$$P_{MUSIC}(\theta_T, \theta_R) = \frac{\boldsymbol{a}^H(\theta_T, \theta_R)\boldsymbol{a}(\theta_T, \theta_R)}{\boldsymbol{a}^H(\theta_T, \theta_R)\boldsymbol{U}_N\boldsymbol{U}_N^H\boldsymbol{a}(\theta_T, \theta_R)}. \tag{12}$$

This MUSIC spectrum reaches peak value when θ_T and θ_R correspond to living-body directions at transmitting and receiving antennas. Therefore, living-body directions at transmitting and receiving antennas, $\theta_{T1} \sim \theta_{TL}$ and $\theta_{R1} \sim \theta_{RL}$ can be estimated by finding peak values of the MUSIC spectrum. Living-body locations can be estimated by finding the intersection of θ_{Tx} and θ_{Rx}.

3. Measurement Conditions

Table 1 and Fig. 2 show measurement conditions and measurement system, respectively. In these measurements, a 4×4 bistatic MIMO configuration was used. As shown in Fig. 2(a), Single-Pole 4 Throw (SP4T) switch was used at transmitting side. A continuous wave (CW) signal at 2.47125 GHz was used, and transmitted power at the antennas was set to 7.0 dBm. The CW signal is shared with the receiver side since accurate synchronization between transmitting and receiving sides is needed. At the receiver side, received signals are input to a down-converter unit by way of Low-Noise Amplifier (LNA) unit. The down-converted baseband signals (I_1, Q_1, ∼ I_4, Q_4) are digitized by data-acquisition unit (DAQ) with a sampling frequency 12.5 kHz. However, the snapshot rate for MIMO channel is determined by the switching speed of SP4T. The transmitter and the receiver arrays consist of four horizontally arranged patch antennas with half wavelength element spacing. A photo of the array is shown in Fig. 2(b). The thickness, width, and height of the transmitting and receiving antennas are 1.6, 255, and 62 mm, respectively. The patch antennas are formed on a PTFE substrate. The array's center was set to h = 1.0 m, the chest height of the subjects. The distance between transmitting and receiving antennas, D, was set to 4.0 m. The directions of the transmitting and receiving array are defined

Table 1 Measurement conditions.

Antenna element (Tx/ Rx)	4 horizontal patch antenna
Element spacing (Tx/ Rx)	0.5λ
Height of antenna, h	1.0 m
Distance between Tx and Rx, D	4.0 m
Frequency	2.47125 GHz
Tx power	7.0 dBm
Channel measurement time	50 s
Snapshot rate	7.0 Hz
Extracting frequency range	f_1 = 0.02 Hz, f_2 = 3.3 Hz

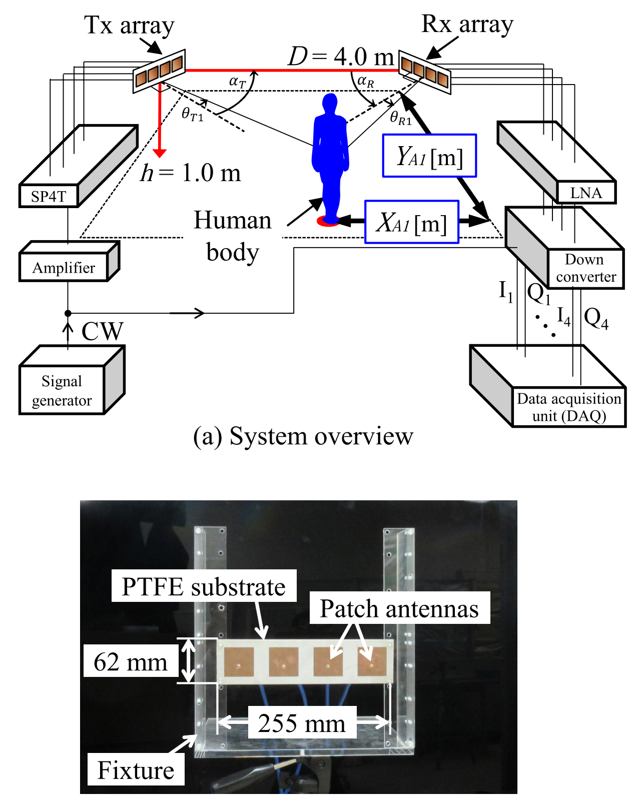

(a) System overview

(b) Array antenna

Fig. 2 Measurement system.

as, α_T and α_R, respectively. As an example, the directions of target 1 from the transmitting and receiving array are shown, too.

Several situations with various numbers of subjects, locations of subjects, were tested. In each trial, the time-variant channels were measured for 50 second periods. The frequency range most strongly influenced by human heart rate runs from 0.6 to 3.3 Hz, while that most strongly influenced by human respiration runs from 0.33 to 0.5 Hz [16]. Also, body sway affects the lower frequency range. Because of this, in this study, f_1 and f_2 were set to 0.02 Hz and 3.3 Hz, respectively. In this approach, living-body location estimation is realized by eliminating the unwanted components and observing only the fluctuating components created by human body motion, heartbeat, and respiration. Note that the rate for taking a snapshot of the MIMO channel is 7.0 Hz, which is mainly determined by switching speed

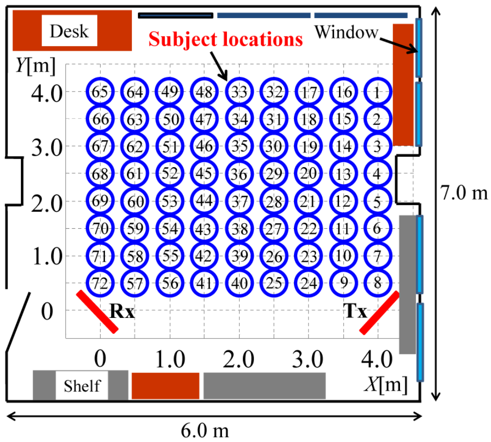

Fig. 3 Measurement environment.

of the transmitting antennas. Even though the exact observation time is not same for all elements in MIMO channel matrix, the time differences in the elements are negligibly short compared to the speed of change in channel caused by living-bodies.

Figure 3 shows the measurement environment. The experiment was carried out in a room containing desks and shelves. The room has concrete walls, and its width, depth, and height are 7.0, 6.0, and 2.7 m, respectively. On one side of the room, there are four windows. The time-variant channels were measured while targets were stationary at (X_{A1}, Y_{A1})~(X_{AL}, Y_{AL}). Here, X_{Ax} and Y_{Ax} are the actual locations at which targets were standing. Subscript x represents target number. Also, target locations are labeled from No. 1 to No. 72. When the receiving antenna is located at the origin and the transmitting antenna is located at $(D, 0)$,the location, (X_{Ax}, Y_{Ax}), is transformed to the angular values by,

$$\theta_{Rx} = -\alpha_R + \tan^{-1}\frac{Y_{Ax}}{X_{Ax}} \tag{13}$$

$$\theta_{Tx} = \alpha_T - \tan^{-1}\frac{Y_{Ax}}{D - X_{Ax}}, \tag{14}$$

where the condition, $Y_{Ax} \geq 0$, needs to be assumed.

As an evaluation criterion of the accuracy, the acceptable error distance is introduced in this study. Since the shoulder width of the subjects is about 0.5 m, 90-th percentile error under 0.5 m is considered as acceptable.

4. Results

Figure 4 shows the time variation of the Single-Input Single-Output (SISO) channel measured with and without a target. When there was a single target, its standing position was No. 37. This SISO channel is the components of the first column of the virtual SIMO channel. This figure indicates that the MIMO channel with a living-body has large time variation compared to that without a living-body. It is found that the MIMO channel is greatly influenced by human body motion.

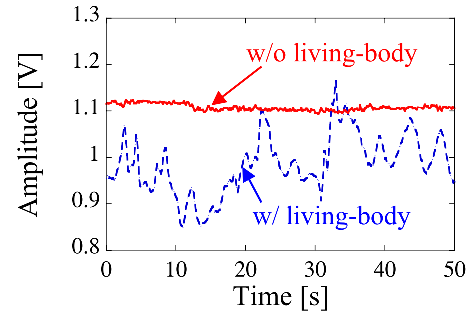

Fig. 4 Time variation of SISO channel.

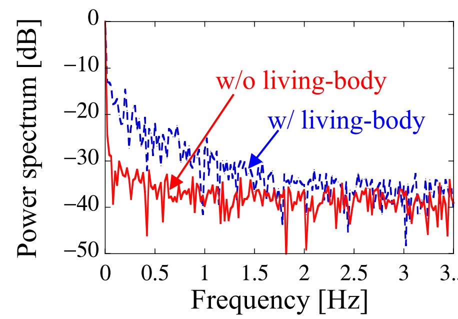

Fig. 5 Frequency response of time-variant SISO channel.

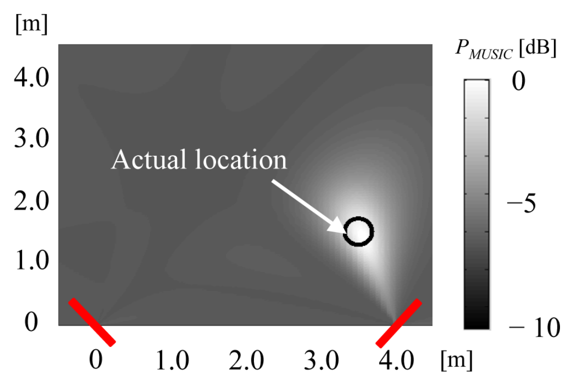

Fig. 6 An example of localization result when one target was present.

Figure 5 shows the frequency response of the time-variant SISO channel measured with and without a target. When there was a single target, the standing position of a single target was No. 37. This figure indicates that the vital sign effects appear at low-frequencies. Accordingly, the fluctuating components from 0.02 to 3.3 Hz were extracted to observe the variation component influenced only by the vital signs. Moreover, it is found that the spectrum with living-body widely spreads. The major reason is body sway and respiration. They cause not only their vibration frequencies but also high-order spurious frequencies.

Figure 6 shows an example of the localization result of the proposed method for a single target standing at position No. 11; i.e. (X_{A1}, Y_{A1}) coordinates of (3.5 m, 1.5 m). As shown in this figure, the peak value of the MUSIC spectrum appears near the actual location of the target. In this case,

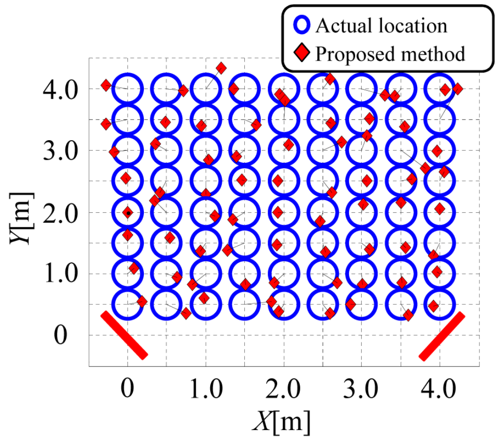

Fig. 7 Localization results from 72 measurement positions when a single target was present.

the estimated location (X_1, Y_1) coordinates were (3.56 m, 1.42 m), so location estimation error was 0.1 m. This result confirms that the living-body localization algorithm works even in multi-path environments.

Figure 7 shows the localization results for a single target at each of the 72 measurement positions. In this figure, the diamonds and circles indicate estimated and actual locations of the target, respectively. This figure confirms that the estimated location lies close to the actual location of the target. Even though the maximum estimation error was 0.55 m, the most of the estimated locations are within acceptable error, i.e. 0.5 m. Therefore, living-body locations can be estimated with high accuracy regardless of target location if the number of target is one.

Figure 8 shows the photo and results of the experiments, where localization accuracy was evaluated for 100 trials with two targets. The photo presents the location of the targets as well as the measurement system, which was explained in the previous section. The standing positions of target 1 and target 2 were No. 21 and No. 52, respectively. Their actual (X_{Ax}, Y_{Ax}) coordinates were (3.0 m, 2.0 m) and (1.0 m, 2.5 m), respectively. As shown, the estimation error is small.

Figure 9 shows localization accuracy results from 100 trials when three targets were present. The (X_{Ax}, Y_{Ax}) coordinates of targets 1, 2 and 3 were (4.0 m, 2.0 m), (2.0 m, 2.0 m), and (0 m, 2.0 m), respectively. Clearly estimation accuracy is degraded compared to the two target case, but the results roughly indicate three target locations. It can be seen that the location error of target 1 is degraded seriously and this is because there is a concrete pillar just next to the target 1 as shown in Fig. 3. It is supposed that this concrete pillar disturbs the reflected signal from target 1. Also, there are several spurious images that stray from the target locations. The main reason is supposed that the reflected signals from multiple targets are strongly correlated incidentally. This can be happened because this MIMO radar observes the Doppler components mainly caused by the respirations, where those behaviors of multiple subjects sometimes become similar.

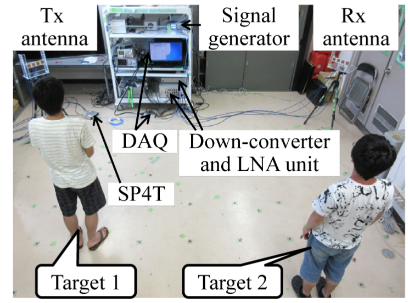

(a) Photo

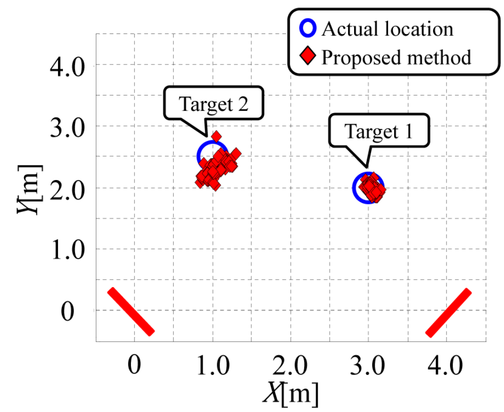

(b) Estimated locations

Fig. 8 Localization accuracy results from 100 trials when two targets were present.

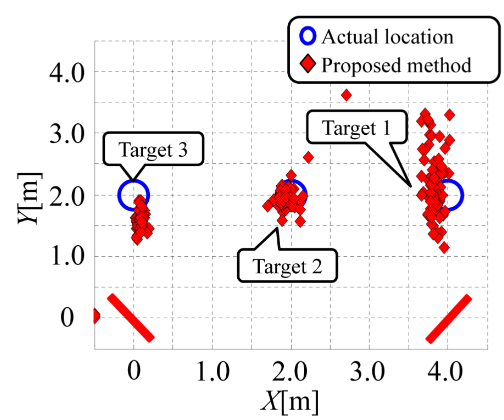

Fig. 9 Localization accuracy results from 100 trials when three targets were present.

Figure 10 shows the Cumulative-Distribution-Function (CDF) of distance error for various numbers of targets. The CDF values shown were obtained by mixing the estimated error of multiple targets. We find that the 90-th percentile error was 0.14 m, 0.32 m, and 0.96 m for one-, two-, and three-target cases, respectively. The error corresponding to three target case exceeds the acceptable accuracy, and the discussion about the accuracy degradation for this case was mentioned in the previous paragraph. It is found multiple living-

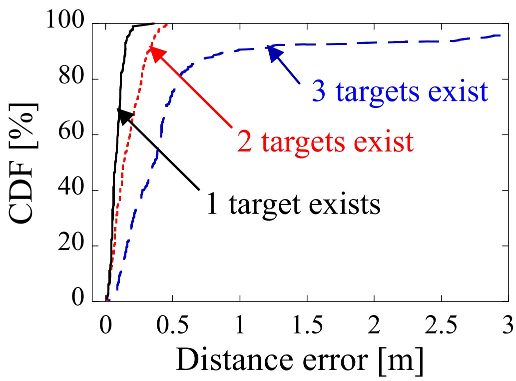

Fig. 10 CDF of distance error with various numbers of targets.

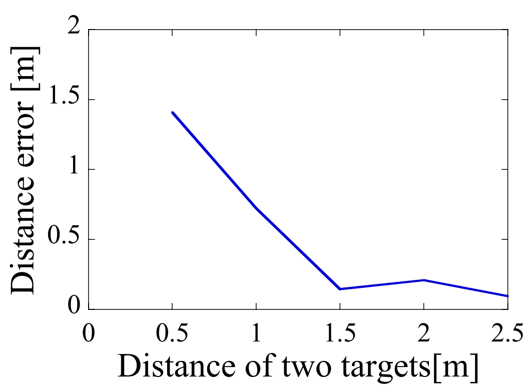

Fig. 11 Distance error with two targets separated by various distances.

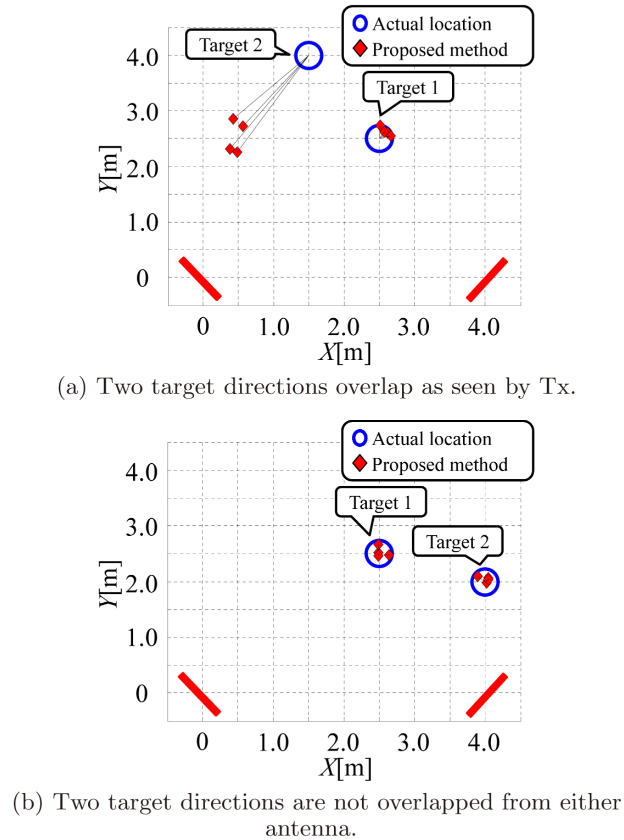

Fig. 12 An example of localization results with two target at various locations.

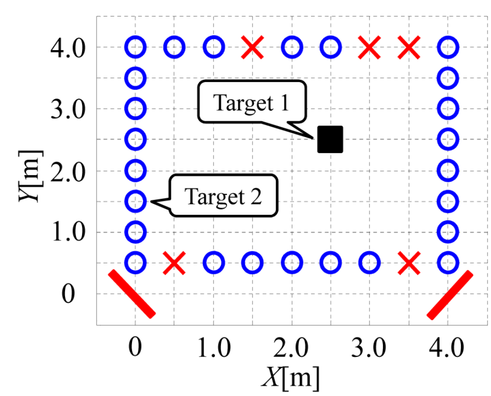

Fig. 13 Localization accuracy evaluation with two targets at various locations.

body locations up to two targets can be estimated with acceptable accuracy, but the estimation error for three targets exceeds the acceptable accuracy. Nevertheless, it is considered the error can be reduced by increasing the observation period or number of the antennas. Though the 90-th percentile location error in [9] is about 0.5 m for the multiple targets up to five, our results are comparable if the number of the target is up to two. Also, it must be noted that we used CW whereas the work [9] uses 1.79 GHz bandwidth.

Figure 11 shows the distance error with two targets separated by various distances. In this measurement, the location of target 1 is fixed at No. 28, and the location of target 2 is varied from No. 37 to No. 44, No. 53, No. 60 and No. 69. The results shown are the average values of the distance errors over 5 estimation trials. As shown, the distance error exceeds 1.0 m when the distance between the two targets is 0.5 m. This occurs because the two peaks in the MUSIC spectrum overlap. However, the estimation accuracy improves a greater separation distances. The distance error held to under 0.5 m when the separation exceeds 1.5 m.

Figure 12 shows an example of the localization results with two targets at various locations. As shown, the estimation accuracy falls when the two target directions are overlap as seen from the transmitting antenna. On the other hand, both target locations are well estimated when the two target directions do not overlap from either antenna.

Figure 13 shows localization accuracy results with two targets at various locations. In this measurement, the MIMO channel was measured while changing the standing position of target 2 in the periphery of the measurement area; target 1 remained stationary at position No. 29. Also, the number of trials for each situation was set to four. In this figure, the circles indicate the cases whose the average value of the distance errors over 4 estimation trials were less than 1.0 m; the x-marks indicates cases with large estimation error. It is found that the proposed method is accurate for most combinations of two target locations.

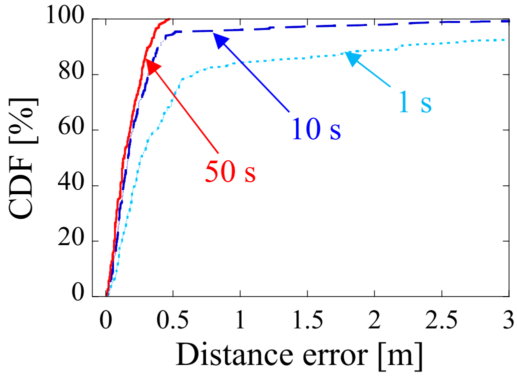

Fig. 14 CDF of distance error with various channel measurement periods.

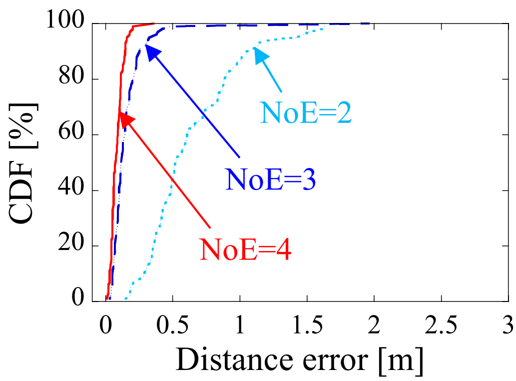

Fig. 15 CDF of distance error with various numbers of antenna elements.

Figure 14 shows the CDF of distance error for various channel measurement periods. The two targets stood at positions No. 21 and No. 52. The channel measurement period was set to 1, 10, and 50 seconds. This figure confirms that the distance error at the 90% value of CDF was 2.1 m, 0.39 m, and 0.32 m for measurement periods of 1, 10, and 50 seconds, respectively. This is because the correlation among the reflected signals from multiple-targets cannot be calculated correctly if the observation period is not sufficient. That is, estimation accuracy is improved by increasing the channel measurement period.

Figure 15 shows the CDF of distance error with various numbers of antenna elements (NoE). The single target stood at position No. 37. As shown in this figure, the distance error at the 90% value of CDF was 0.14 m, 0.25 m, and 1.1 m at NoE values of four, three and two, respectively. Clearly the estimation accuracy is degraded significantly when the number of antenna elements is two. This is because the number of eigenvectors used in the MUSIC spectrum is decreased by decreasing the number of antenna elements. Therefore, estimation accuracy is improved by increasing the number of antenna elements.

5. Conclusion

This paper has proposed a method of estimating living-body locations by using bistatic MIMO radar in multi-path environments. Living-body direction at the transmitter and the receiver are estimated by applying MUSIC to the Doppler-shifted channel created by movement of the living-body, and localization is performed by finding the intersection point of these two directions.

Experiments confirmed that the maximum estimation error of this method was 0.55 m for a single target standing in 72 measurement positions. Also, the estimation error at the 90% value of CDF for two and three targets was 0.32 m and 0.96 m, respectively. Furthermore, it was confirmed that the estimation error was held to less than 0.5 m when two targets are separated by more than 1.5 m. Moreover, it was found that the estimation accuracy was improved by increasing the channel measurement period and increasing the number of antenna elements. These results confirm that the proposed method can accurately estimate the locations of living-bodies even in multi-path environments.

Acknowledgements

This research was partially supported by the Telecommunications Advancement Foundation.

References

[1] H. Seki and Y. Hori, "Detection of abnormal action using image sequence for monitoring system of aged prople," IEEJ Trans. Industry Applications, vol.122, no.2, pp.182–188, Feb. 2002.

[2] A. Mase, N. Ito, Y. Komada, A. Kobayashi, T. Maruyama, H. Shimazu, E. Sakata, and F. Sakai, "Microwave reflectometric measurement of heart-rate variability and stress evaluation," Asia-Pacific Microwave Conference, Kaohsiung, pp.625–627, Dec. 2012.

[3] Y.J. An, B.J. Jang, and J.G. Yook, "Detection of human vital signs and estimation of direction of arrival using multiple Doppler radars," J. Korean Institute of Electromagnetic Engineering and Science, vol.10, no.4, pp.250–255, Dec. 2010.

[4] J.C. Lin and J. Salinger, "Microwave measurement of respiration," 1975 IEEE-MTT-S International Microwave Symposium (MTT-S), pp.285–287, May 1975.

[5] D. Nagae and A. Mase "Measurement of heart rate variability and stress evaluation by using microwave reflectometric vital signal sensing," Review of Scientific Instruments, vol.81, no.9, 094301, 2010.

[6] A. Droitcour, V. Lubecke, J. Lin, and O. Boric-Lubecke, "A microwave radio for Doppler radar sensing of vital signs," 2001 IEEE International Microwave Symposium (MTT-S), vol.1, pp.175–178, May 2001.

[7] H. Avagyan, A. Hakhoumian, H. Hayrapetyan, N. Pogosyan, and T. Zakaryan,"Portable non-contact microwave Doppler radar for respiration and heartbeat sensing," Armenian Journal of Physics, vol.5, no.1, pp.8–14, 2012.

[8] M. Nango, N. Honma, K. Nishimori, and H. Sato, "Biological activity detection method using MIMO system," IEICE Communications Express, vol.2, no.2, pp.36–41, 2013.

[9] F. Adib, Z. Kabelac, and D. Katabi, "Multi-person motion tracking via RF body reflections," Computer Science and Artificial Intelligence Laboratory Technical Report, MIT-CSAIL-TR-2014-008, April 2014.

[10] J. Li and P. Stoica, MIMO Radar Signal Processing, Wiley, Hoboken, NJ, USA, 2008.

[11] K. Konno, M. Nango, N. Honma, K. Nishimori, N. Takemura, and T. Mitsui, "Experimental evaluation of estimating living-body direction using array antenna for multi-path environment," IEEE Anten-

nas Wireless Propag. Lett., vol.13, pp.718–721, April 2014.

[12] R.O. Schmidt, "Multiple emitter location and signal parameter estimation," IEEE Trans. Antenna Propagation, vol.AP-34, no.3, pp.276–280, March 1986.

[13] D. Sasakawa, K. Konno, N. Honma, K. Nishimori, N. Takemura and T. Mitsui, "Localizing living body using bistatic MIMO radar in multi-path environment," 8th European Conference on Antennas and Propagation (EUCAP 2014), Electric Proc. EuCAP 2014, pp.3863–3867, April 2014.

[14] K. Konno, N. Honma, D. Sasakawa, Y. Tsunekawa, K. Nishimori, N. Takemura, T. Mitsui, and Y. Tsunekawa "Localizing multiple target using bistatic MIMO radar in multi-path environment," 2014 IEEE International Workshop on Electromagnetics: Applications and Student Innovation Competition (iWEM 2014), vol.2, pp.90–91, Aug. 2014.

[15] N. Honma and K. Nishimori, "Using multiple antenna systems for living-body sensing," IEICE Trans. Commun. (Japanese Edition), vol.J98-B, no.9, pp.853–867, Sept. 2015.

[16] J.M. Park, D.H. Choi, and S.O. Park, "Wireless vital signal detection systems and its applications at 1.9 GHz and 10 GHz," 2003 IEEE/Antennas and Propagation Society International Symposium, vol.4, pp.747–750, June 2003.

Keita Konno received the B.E. in electrical and electronic engineering from Iwate University, Morioka, Japan in 2013. He is currently with NTT east corporation.

Naoki Honma received the B.E., M.E., and Ph.D. degrees in electrical engineering from Tohoku University, Sendai, Japan in 1996, 1998, and 2005, respectively. In 1998, he joined the NTT Radio Communication Systems Laboratories, Nippon Telegraph and Telephone Corporation (NTT), in Japan. He is now working for Iwate University. He received the Young Engineers Award from the IEICE of Japan in 2003, the APMC Best Paper Award in 2003, the Best Paper Award of IEICE Communication Society in 2006, and the APMC2014 Prize in 2014, respectively. His current research interest is MIMO antenna system and its applications. He is a member of IEEE.

Dai Sasakawa received the B.E. in electrical and electronic engineering from Iwate University, Morioka, Japan in 2014. He is currently in the master program in Iwate University. His research interest is array antenna calibration for living-body radar. He received IEEE Sendai Section Best Paper Prize in 2014.

Kentaro Nishimori received the B.E., M.E. and Ph.D. degrees in electrical and computer engineering from Nagoya Institute of Technology, Nagoya, Japan in 1994, 1996 and 2003, respectively. In 1996, he joined the NTT Wireless Systems Laboratories, Nippon Telegraph and Telephone Corporation (NTT), in japan. He was senior research engineer on NTT Network Innovation Laboratories. He is now associate professor in Niigata University. He was a visiting researcher at the Center for Teleinfrastructure (CTIF), Aalborg University, Aalborg, Denmark from Feb. 2006 to Jan. 2007. He was an Associate Editor for the Transactions on Communications for the IEICE Communications Society from May 2007 to May 2010 and Assistant Secretary of Technical Committee on Antennas and Propagation of IEICE from June 2008 to May 2010. He received the Young Engineer Award from IEEE AP-S Japan Chapter in 2001, Best Paper Award of Software Radio Society in 2007 and Distinguished Service Award from the IEICE Communications Society in 2005, 2008 and 2010. His main interests are spatial signal processing including MIMO systems and interference management techniques in heterogeneous networks. He is a member of IEEE. He received IEICE Best Paper Award in 2010.

Nobuyasu Takemura received B.E., M.E. and Ph.D. degrees in electrical engineering from Tokyo University of Science, Tokyo, Japan, in 1996, 1998 and 2010, respectively. From 1998 to 2007, he joined the Information Technology Research and Development Center of Mitsubishi Electric Corporation, Japan. From 2007 to 2014, he joined the ET Center of Samsung R&D Institute Japan. He is currently associate professor in Nippon Institute of Technology. His research interests are antennas for mobile communication systems, MIMO systems, satellite communication systems, and radar systems. Dr. Takemura received the Young Investigators Award from the Institute of Electronics, Information and Communication Engineers (IEICE) of Japan in 2003. He is a member of the IEEE.

Tsutomu Mitsui received the B.E. degrees from Musashi Institute of Technology, Tokyo, Japan, in 1987. In 1987, he joined Tokyo Keiki Inc., Tokyo, Japan. Since 1999, he has been with the Samsung R&D Institute Japan. His current research interest is array antenna systems.

Yoshitaka Tsunekawa received the B.E. degree from Iwate University, Morioka, Japan, in 1980 and the M.E. and the Doctor of Engineering degrees from Tohoku University, Sendai, Japan, in 1983 and 1993, respectively. Since 1983, he has been with the Faculty of Engineering, Iwate University, where he is now a professor at the Department of Electrical Engineering and Computer Science. His current research interests include digital signal processing and digital control. He is a member of the Institute of Electronics, Information and Communication Engineers of Japan, and IEEE.